



# Analytic investigation of climate stability on Titan: sensitivity to volatile inventory

Ralph D. Lorenz<sup>a,\*</sup>, Christopher P. McKay<sup>b</sup>, Jonathan I. Lunine<sup>c</sup>

<sup>a</sup>*Lunar and Planetary Laboratory, University of Arizona, Tucson, AZ 85721-0092, USA*

<sup>b</sup>*NASA Ames Research Center, Moffett Field, CA, USA*

<sup>c</sup>*Reparto di Planetologia, CNR Istituto di Astrofisica Spaziale, 00133, Rome, Italy*

Received 24 November 1998; received in revised form 19 March 1999; accepted 14 April 1999

## Abstract

We develop a semiempirical grey radiative model to quantify Titan's surface temperature as a function of pressure and composition of a nitrogen-methane-hydrogen atmosphere, solar flux and atmospheric haze. We then use this model, together with non-ideal gas-liquid equilibrium theory to investigate the behavior of the coupled surface-atmosphere system on Titan. We find that a volatile-rich Titan is unstable with respect to a runaway greenhouse—small increases in solar luminosity from the present value can lead to massive increases in surface temperature. If methane has been photolyzed throughout Titan's history, then this runaway can only be avoided if the photolytic ethane is removed from the surface-atmosphere system. © 1999 Elsevier Science Ltd. All rights reserved.

## 1. Introduction and previous work

In this paper, we examine the behavior of the surface-atmosphere system on Titan, where both the main atmospheric constituents, nitrogen and methane, are condensible greenhouse gases. By combined study of the surface-atmosphere thermodynamic equilibrium with radiative equilibrium of the resultant atmosphere, self-consistent climate states can be found and their stability investigated. Further, since Titan's volatile inventory has evolved through time, certainly by methane photolysis and perhaps by volcanic delivery of methane and other gasses, some possible climate histories of Titan can be constructed.

Implicit in this work is the assumption that the atmosphere as a whole is in saturation equilibrium with a surface reservoir: this assumption, while demonstrably incorrect for the present Earth (see e.g. Kasting et al., 1988 for a discussion) is the only practicable one

for studying coupled ocean-atmosphere systems on a planetary scale (Kuramoto and Matsui, 1994; Kasting et al., 1988; Nakajima et al., 1992; McKay et al., 1993; Ingersoll, 1969; Dubouloz et al., 1989 etc.). In reality, while the methane will be close to saturation just over the liquid surface (Flasar, 1983), transport by winds over dry land and loss by precipitation means that, as on Earth, large regions may be out of equilibrium. However, without data to constrain these processes, the assumption of equilibrium is a reasonable and consistent basis on which to compare different cases.

The methane in Titan's atmosphere is destroyed by photolysis on short timescales ( $\sim 10^6$  years, see Yung et al., 1984; Lara et al., 1994, 1996; Toublanc et al., 1995)—mainly through conversion into ethane—its presence in the present epoch implies a resupply mechanism and/or buffering by a surface or near-surface reservoir. Thus we consider that a reservoir of ethane, methane and nitrogen is in thermodynamic equilibrium with the atmosphere, although the reservoir may in part be subsurface (Eluskiewicz and Stevenson, 1990; Kossacki and Lorenz, 1995).

There is some indirect evidence of a surface methane reservoir in near-IR observations using the Hubble

\* Corresponding author. Tel.: +1-520-621-5585; fax: +1-520-621-4933.

E-mail address: rlorenz@lpl.arizona.edu (R.D. Lorenz).

Space Telescope (Smith et al., 1996), and groundbased speckle imaging (Gibbard et al., 1999). These observations indicate a number of dark areas whose surface reflectivity has been determined to be close to zero—entirely consistent with deposits of liquid hydrocarbons (principally methane and ethane) on the surface, and difficult to account for by anything else. Furthermore, the revised values of the disk-integrated radar reflectivity of Titan (Muhleman et al., 1995) are quite low—less than 0.1—and are compatible with a mixed ice-hydrocarbon surface (see Lorenz and Lunine, 1997 for a discussion).

It may be noted (Lorenz, 1998) that a typical distribution of craters on Titan's surface would cover only about 10% of Titan's surface area, yet could hold the equivalent of 350 m global depth of liquid (i.e. roughly 3 bar of volatiles). Furthermore, a single large (300 km diameter) crater basin could hold a volume equivalent to 30 m global depth even if it were relaxed to only 5 km deep (a depth/diameter ratio of less than 1%): such a crater covers only one or two pixels in HST or speckle images. Additionally, very large basins which could hold several bars worth of volatiles would be likely, by virtue of their effects on the planetary moments of inertia, to be located at the poles where they cannot yet be observed from Earth: the South Pole Aitken basin on the moon, and the large impact crater on the asteroid Vesta are in polar locations. There is also evidence that the north polar region of Mars is a large basin which may once have held a water ocean. Although none of these considerations prove that Titan has a large volatile reservoir, they do underscore that such a reservoir may be present, despite the observational evidence against the canonical 'global ocean' suggested by Lunine et al. (1983). It may be noted also that the isotopic composition (and specifically the  $\text{CH}_3\text{D}/\text{CH}_4$  ratio) are consistent with enrichment due to photolysis of methane throughout Titan's history (Lunine et al., 1999).

For this study, the morphological details of the reservoir, whether surface, subsurface or both, are not important, only that it is in thermodynamic equilibrium with the atmosphere.

Lunine and Rizk (1989), Lunine and Stevenson (1985) and McKay et al. (1993) pointed out the implications of the solar luminosity and methane destruction processes on Titan's volatile reservoir and climate through time. We extend the work of the latter by examining the climatic stability of the ocean-atmosphere system not only for volatile inventories that could be in equilibrium with the present Titan atmosphere, but also for large initial volatile inventories that could have evolved into the present one (i.e. with less ethane and more methane, reflecting the irreversible change of the latter into the former).

We have devised a semiempirical model for computing Titan's surface temperature over a wide range of

conditions; this model is validated and parameters chosen by tuning to fit the results of the detailed non-grey radiative-convective model of McKay et al. (1989). While computationally it would be possible to use the latter model directly in the work that follows, the semiempirical model allows better visibility into the parametric sensitivity of Titan's climate, and is considerably more convenient to use since the climate stability investigation requires that the ocean thermodynamics and the radiative equilibrium be solved iteratively for self-consistent solutions.

Some volatile inventories are stable—the atmosphere above an ocean at some temperature provides sufficient greenhouse warming to keep the ocean at that temperature. Some inventories are not—insufficient warming makes the ocean colder, the atmospheric pressure falls producing less warming still, and so on—an atmospheric collapse. Similarly, a runaway greenhouse can occur, where increased radiative warming feeds back through the ocean-atmosphere equilibrium to produce yet more warming, until the ocean has the volatiles boiled out of it. Hysteresis is evident in these cases—the runaway greenhouse is not reversed by a small drop in solar luminosity.

## 2. Ocean–atmosphere composition: model

The volatile inventory on Titan's surface will divide itself between the atmosphere and surface deposits ('ocean': at the present epoch, the non-gas component of the volatile inventory is above the melting point of all possible compositions). 'Ocean' may mean dispersed lakes and seas as suggested by the imaging data, and/or fluids in pore space in the crust—an 'aquifer'—although there are at present no direct constraints on such a reservoir.

The partial pressure  $p_i$  of a component must be less than or equal to  $M_{ig}$  where  $M_i$  is the mass per unit area of species  $i$ , and  $g$  is Titan's surface gravity. We use the formalism of Thompson (1985), as modified by McKay et al. (1993) to determine the partitioning of gas between the ocean and atmosphere (Kouvaris and Flasar, 1991 present a more complex and accurate representation, but the simplified McKay/Thompson formalism is sufficiently accurate for our purposes) see also Thompson et al. (1992). Essentially the pressures are determined by Raoult's law and Henry's law, with  $p_i$  of a component  $i$  equal to its saturation vapor pressure  $P_{s_i}$  multiplied by its mole fraction in the ocean  $X_i$  and by an activity coefficient  $\gamma_i$  which accounts for the non-ideal behavior of the various components, described in turn by interaction parameters  $\alpha_{ij}$  and  $m_{ij}$  corresponding to the interaction of components  $i$  and  $j$ . So

$$p_i = \gamma_i P_{s_i} X_i \quad (1)$$

Table 1  
Thermodynamic parameters used to determine vapor pressures above ocean

<i>j</i>	Ethane	Nitrogen	Methane
$\alpha(i = \text{CH}_4) \text{ K}$	55.3	156	–
$\alpha(i = \text{N}_2) \text{ K}$	217.6	–	53.1
$m(i = \text{CH}_4)$	2	2	–
$m(i = \text{N}_2)$	1	–	2
<i>A</i> bar	–	13,000	35,454
<i>B</i> K	–	728.8	1145.7

with

$$\ln(\gamma_i) = \frac{1}{T} \sum_{i \neq j} \alpha_{ij} X_j^{m(i,j)} \quad (2)$$

and

$$P_{s_i} = A_i \exp(-B_i/T) \quad (3)$$

The constants used in the equations above are listed in Table 1. Note that throughout this work, when we indicate a ‘saturation vapor pressure’ we refer to the saturation vapor pressure of a pure compound. When we indicate the partial pressure or vapor pressure of a component in a mixture we refer (since we consider equilibrium) this to be the saturation vapor pressure of that component of the specified mixture.

For a given volatile inventory  $M_i = 1, 2, 3$  and temperature  $T$ , it is first assumed that all the components are condensed, i.e. that the fraction in the condensed phase  $F_i$  of each species is 1. The partial pressures are computed using the equations above, and  $F_i$  reduced accordingly. The computation is repeated until the partial pressure of the species given by  $M_i(1-F_i)g$  and that given by Eq. 1 above converge.

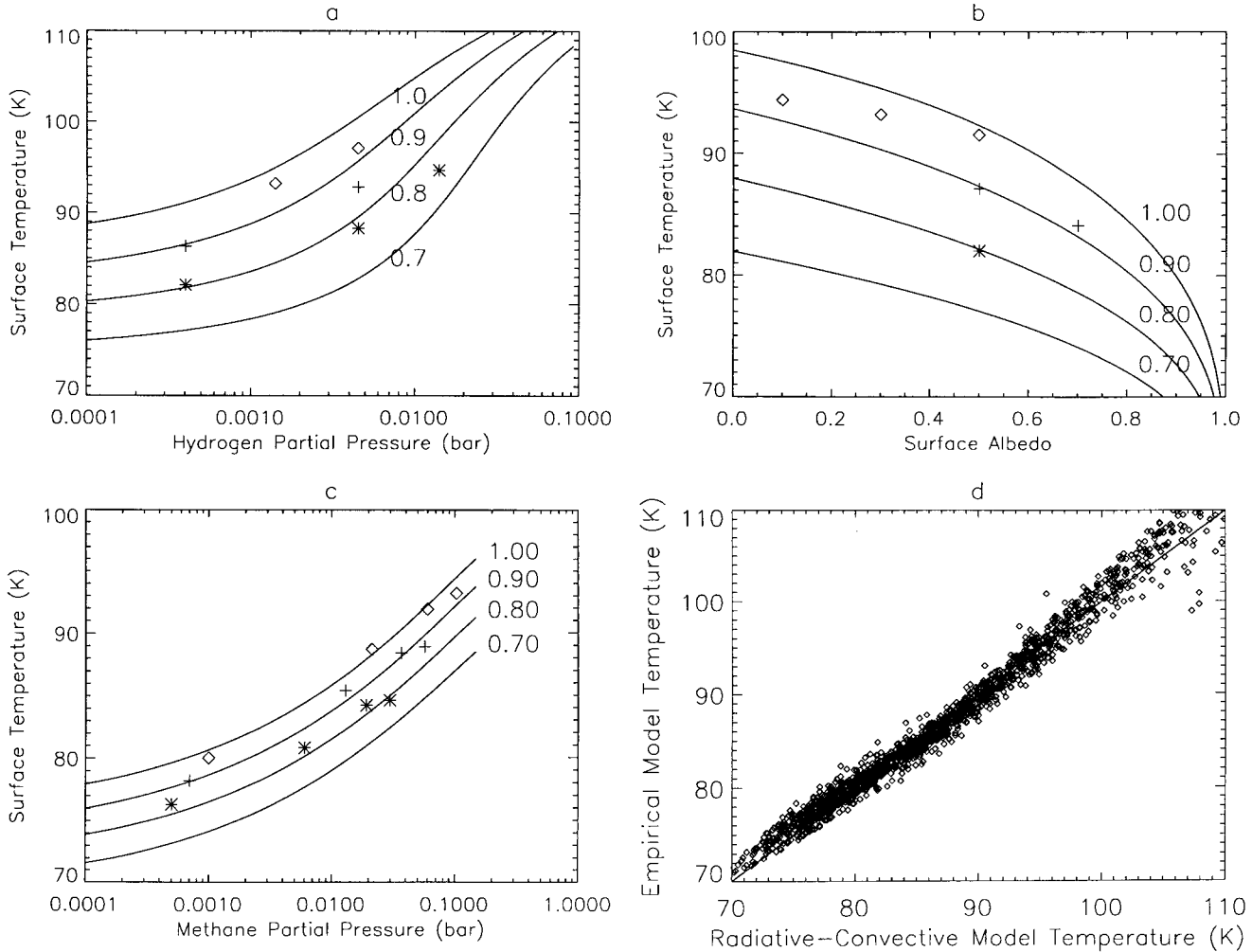


Fig. 1. Results of the simple model of Titan’s radiative balance surface temperature compared with the results from the McKay et al. radiative-convective model. (a)–(c) Analytic results are the lines, labeled by the value of solar luminosity, with varying hydrogen abundance, surface albedo and methane partial pressure, respectively. Symbols indicate radiative-convective results, diamonds for  $S = 1$ , plus signs for  $S = 0.9$  and asterisks for  $S = 0.8$ . (d) All results of the radiative-convective model with the corresponding estimate from the empirical model. The correlation coefficient is 0.989 and the RMS error is 1.5 K.

The vapor pressure of ethane at the temperatures of interest is negligible. Thus all the ethane remains as a liquid. Nitrogen, on the other hand, is the most volatile component, and to first order a methane-poor volatile mixture has an atmospheric pressure equivalent to the mass of nitrogen (since ethane and nitrogen do not significantly interact), or the saturation vapor pressure of nitrogen at that temperature, whichever is the smaller.

Adding methane makes the situation more complicated. It is less volatile than nitrogen. Furthermore, nitrogen dissolves in it. This leads to the somewhat counterintuitive effect that, depending on the other parameters, adding methane to the system can reduce the atmospheric pressure (just as adding a drop of water to a flask full of ammonia gas will lower its pressure, since much of the ammonia dissolves instantly in the water).

### 3. Constraints on volatile inventory

As indicated above, the volatile inventory divides itself between the atmosphere and surface or subsurface deposits which we assume are in equilibrium with the atmosphere. Concerning the latter, we have a considerable body of data on the atmosphere immediately above the surface from the Voyager 1 and 2 encounters, specifically from the radio-occultation experiment (Lindal et al., 1983) and at higher altitudes from the IRIS infrared spectrometer. A combined analysis was undertaken by Lellouch et al. (1989).

We allow the total surface pressure to vary between 1.4 and 1.5 bar: although some engineering models have been constructed (Yelle et al., 1997) which allow surface pressures between 1.35 and 1.61 bar, we believe this range is too great, as these models were devised to conservatively determine the density at high altitude. The two cases shown in Fig. 1 are compatible with the constraints described above.

A recent re-analysis of IRIS data by Samuelson et al. (1997) suggested that the near-surface temperature is  $93.8 \pm 1$  K, and the methane mole fraction is 5.7%. The corresponding value of methane relative humidity (since the saturation vapor pressure of pure methane at 94 K is 0.177 bar) is about 60%, a value consistent with previous estimates. These are low-latitude values: Samuelson et al. (1997) find temperatures about 3 K lower at  $\pm 60^\circ$  latitude, and methane mole fractions about a factor of 2 lower. However, since this interpretation of high-latitude Voyager data is not universally accepted, and since the incident sunlight at high latitudes is small (so a global average heat balance calculation allocates high weighting to low-latitude values) we use the low-latitude figures as our 'global' values.

In the analysis that follows, we neglect the role of Argon. Thermodynamically and radiatively, it behaves similarly to nitrogen. In the analysis of Lellouch et al. (1989) the role of Argon was primarily that of increasing the relative molecular mass of the gas near the surface: a larger argon abundance requires a larger methane abundance and/or a higher surface temperature in order to match the radio-occultation data. Strobel et al. (1993) derive an upper limit of 10% in argon abundance from analysis of Voyager UVS data.

An immediate result of the observations is that the volatile inventory is at least that observed in the atmosphere, i.e.  $\sim 1.3$  bar  $N_2$  and 0.09 bar  $CH_4$ . Note that in this paper, we assume that all atmospheric inventories can be represented by the surface pressure multiplied by mole fractions for the near-surface atmosphere. As the methane mixing ratio varies with altitude (see e.g. McKay et al., 1997), this is not strictly correct: assuming a 'realistic' mixing ratio profile varying from 6% at the surface to 2% at 40 km, our simplification leads to a 19% overstatement of the inventory. However, the mixing ratio profile is not constrained by Voyager to better than a factor of two, so we retain our uniform one for convenience in our analysis.

Given the limits on methane abundance near the surface from Samuelson et al. (1997) of  $5.7 \pm 1\%$  mole fraction, and an uncertainty of  $\pm 1$  K on the surface temperature, it is possible to determine the approximate relative mix of ethane, methane and nitrogen allowed on Titan's surface, although not their absolute abundance. For example, a volatile-poor case ('lakes', in McKay et al., 1993) could yield the observed atmosphere—and only a trace of surface liquid—with 1.3 bar of nitrogen and as little as 0.09 bar of methane, if no surface ethane is present. Since ethane is observed in the atmosphere, some is likely on the surface and the required methane inventory must be increased to compensate for that which is dissolved in the ethane—e.g. if there is 0.1 bar of ethane, around 0.3 bar of methane is required. If the ethane amount indicated by photochemical models is on the surface, i.e. about 6 bar, then 3–8 bar of methane is required, with 2–3 bar of nitrogen.

### 4. Greenhouse/antigreenhouse model

Titan's atmosphere may be considered, approximately, as a hazy stratosphere (optically thick, but IR-transparent) overlaying a troposphere of greenhouse gases (largely transparent to sunlight, but thick to IR). An analytical model was developed by Samuelson (1983) and a more sophisticated numerical model was developed by McKay et al. (1989). This numerical model allows detailed exploration of the vertical struc-

Table 2  
Parameter ranges used for fit to radiative-convective model

Parameter	Present value	Value 3.5 Gyr ago	Range used in fit
$S$	1.0	0.75	0.8–1.0
$p(\text{N}_2)$ bar	1.4	1.4	0.8–2.0
$p(\text{CH}_4)$ bar	0.9	unconstrained	0.0–1.0
$p(\text{H}_2)$ bar	0.0016	0.0032	0.0–0.01
$P_{\text{H}} \times 3.5 \times 10^{-14} \text{ g cm}^{-2} \text{ s}^{-1}$	0.3	0.6	0.1–0.6
$A_{\text{s}}$	0.2	0.2	0.1–0.8

ture of haze opacity etc., but is somewhat cumbersome for a parametric study of climate.

We therefore use a semiempirical model to determine the surface temperature as a function of atmospheric pressure and composition, haze production, surface albedo and insolation. We describe the model as semi-empirical because, although many parameters and indices are empirically determined, the form of the model is based on an analytical greenhouse/antigreenhouse model of McKay et al. (1999) (see also Lorenz et al., 1997a), based in turn on the classical grey radiative equilibrium, and has the form

$$\sigma T_{\text{s}}^4 = [F_{\text{g}} + (1 - \gamma)(1 - A_{\text{s}})^p F_{\text{a}}] \left( q + \frac{3\tau}{4} \right) + \frac{F_{\text{a}}\gamma}{2} \quad (4)$$

with  $\sigma$  the Stefan–Boltzmann constant,  $T_{\text{s}}$  the surface temperature,  $F_{\text{g}}$  the geothermal heat flux (assumed zero), the parameter  $\gamma$  is the fraction of sunlight absorbed by the haze layer,  $F_{\text{a}}$  is the sunlight absorbed by Titan, with  $F_{\text{a}} = (1 - A)SF_{\text{o}}$  where  $S$  is the insolation relative to the present,  $F_{\text{o}}$  is the present solar constant averaged over Titan's area ( $3.7 \text{ Wm}^{-2}$ ) and  $A$  is the Bond albedo (0.30).  $A_{\text{s}}$  is the surface reflectivity. Note that the Bond albedo is the fraction of sunlight reflected away from the top of Titan's atmosphere: we assume this is independent both of the surface reflectivity (broadly true, except of course in the methane windows in which Titan's surface has been imaged: however, these represent a tiny fraction of the total solar flux) and of the haze opacity: Fig. 6 of McKay et al. (1989) shows that as the haze production is increased, the long-wavelength geometric albedo increases, while the short wavelength albedo decreases. We assume these effects roughly cancel out.  $p$  and  $q$  are empirical constants, with values 0.2 and 0.9, respectively.

In the classical grey approximation, the value of  $p$  would be 1: any light penetrating the haze reaches the surface, and a fraction is absorbed with the rest reflected back to space. The lower value in this empirical formulation reflects the fact that the surface temperature is only weakly dependent on surface reflectivity: much of the red and near-IR sunlight that penetrates through the haze is absorbed by methane in

the troposphere. Similarly, the classical grey approximation has  $q = 0.5$  for the atmosphere at a given optical depth, and  $q = 1.0$  for an absorbing surface. The real Titan, where some light is absorbed in the troposphere and some by the surface, has a value between these two.

$\tau$  is the thermal optical depth of the atmosphere, which we find is well-modelled by

$$\tau = \tau_1 + 6.66(p\text{H}_2)^{0.4}\tau_1 \quad (5)$$

with

$$\tau_1 = 2.87[(p\text{CH}_4)^{0.35}(p\text{N}_2)^{0.65}] \quad (6)$$

$p\text{N}_2$ ,  $p\text{CH}_4$ ,  $p\text{H}_2$  are the partial pressures in bars of nitrogen, methane and hydrogen in the atmosphere. The formulation above reproduces the significant role of the hydrogen abundance, and the stronger effect of hydrogen in thicker atmospheres (pressure-induced absorption by  $\text{H}_2\text{--N}_2$  pairs fills a window region around  $500 \text{ cm}^{-1}$ ) and yields  $\tau \sim 2$  for present conditions. This is approximately the Rosseland mean opacity for the present atmosphere. The stronger dependence of the optical depth on nitrogen rather than methane should be noted:  $\text{N}_2\text{--N}_2$  and  $\text{N}_2\text{--CH}_4$  are the dominant contributors to opacity, while  $\text{CH}_4\text{--CH}_4$  is less important—see Courtin et al. (1995) and McKay et al. (1989). Physically, Eq. (6) is inapplicable for very low methane abundances—if  $p\text{CH}_4$  is zero, the formula would predict zero opacity, even if there were vast amounts of nitrogen. However, we tried variants of the form  $t = Ap\text{N}_2^a + Bp\text{CH}_4^b + Cp\text{CH}_4^c p\text{N}_2^d$  with  $a$ – $d$ ,  $A$ ,  $B$ ,  $C$  constants, but the fits to the data were in fact poorer than the simple form above. Thus, with the caveat that our model applies strictly only to atmospheres with at least a trace of methane, we retain Eq. 6 in the form indicated above.

We express  $\gamma$  as

$$\gamma = 1 - e^{-\tau_{\text{v}}} \quad (7)$$

with  $\tau_{\text{v}}$  the effective haze optical depth given by,

$$\tau_{\text{v}} = 0.78P_{\text{H}}^{0.5}S^{0.25}p^{0.33} \quad (8)$$

with  $P_{\text{H}}$  the haze production rate in units of

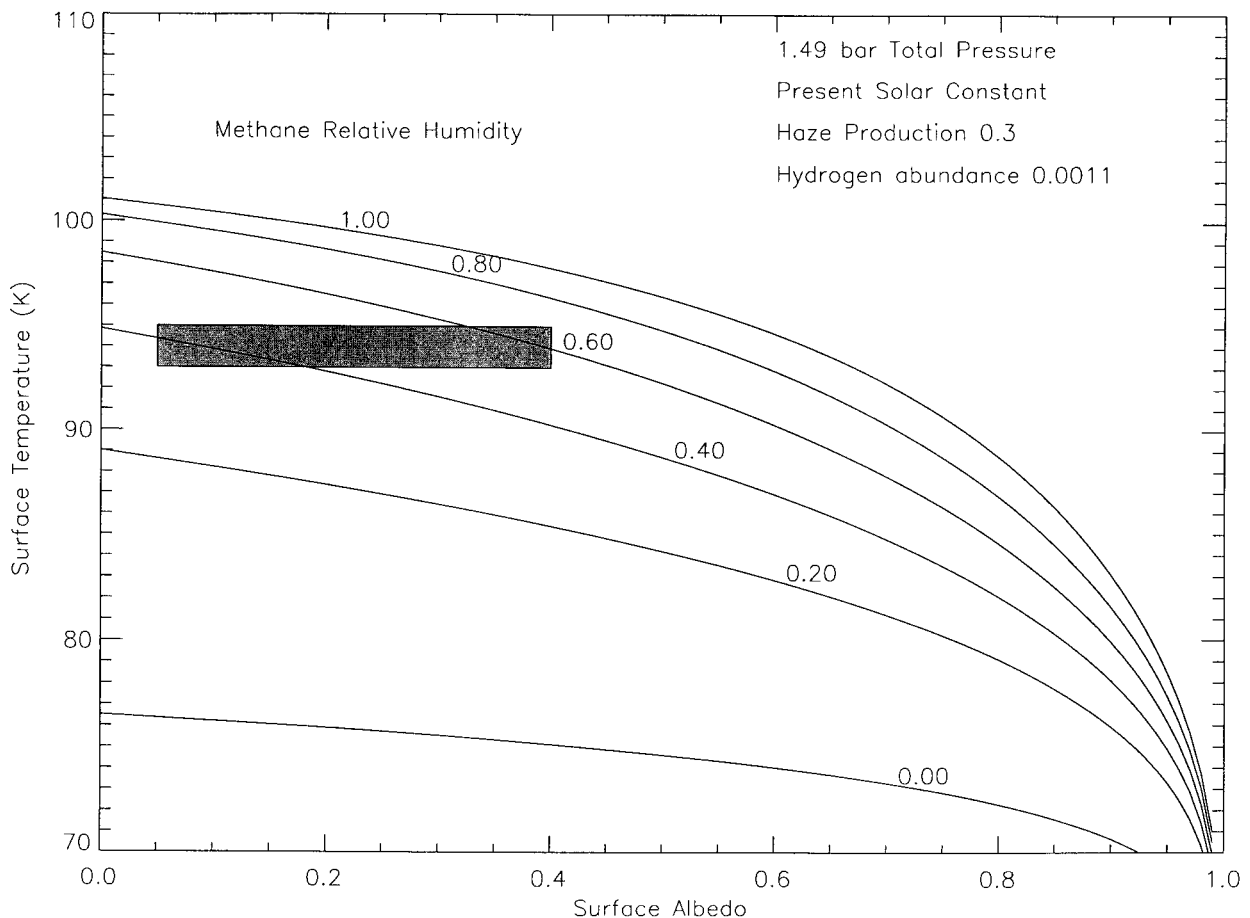


Fig. 2. The surface albedo is varied, for fixed values of relative humidity of methane. The surface temperature is more sensitive to surface albedo for high values of that parameter, especially for high humidity values. The shaded box indicates the observed limits on the surface reflectivity, and the surface temperature derived from Voyager observations. It can be seen that only humidities of 40–60% are compatible with the observed temperature—in good agreement with Samuelson et al.'s (1997) estimate of ~6% mole fraction.

$3.5 \times 10^{-14} \text{ g cm}^{-2} \text{ s}^{-1}$ . The dependence on insolation and total surface pressure  $p$  are due to the column depth of the haze being a function of the total pressure of the atmosphere (since the haze is produced at a fixed pressure  $\sim 10^{-4}$  bar) and of the scale height. The scale height roughly depends principally on temperature, which in turn depends on  $S^{0.25}$ . In a simple atmosphere with haze descending to the surface,  $\tau_v$  might be expected to be proportional to the number of scale heights below the production altitude (i.e. to surface pressure)—the lower power for pressure in this empirical fit may indicate the role of condensation in removing the lower layers of haze.

The constants in the expressions above were optimized using the simplex method to fit a set of 1660 runs of the McKay et al. (1989) nongrey radiative-convective model of Titan's atmosphere, with parameters varied as described in Table 2. The results are shown in Fig. 1: the expressions above reproduce the results of the radiative-convective model with a root-mean squared error of 1.5 K.

While the agreement is not perfect (and some systematic error is present at very low and very high temperatures), it is adequate for the present purposes and is commensurate with the probable accuracy of the nongrey model. The above expressions are simple enough to allow a mental feel for the parametric sensitivity, yet also have some physical sense, unlike a purely empirical relation. We do not believe a simpler set of expressions could reproduce the temperature over such a wide range of conditions, although other relationships with equal complexity might be able to do so.

## 5. Parameter selection

The surface albedo is assumed to be  $\sim 0.2$  at present, although as Lorenz and Lunine (1997) and Lorenz et al. (1997b) point out, values between 0.0 and 0.4 are compatible with the present temperature balance, largely because so little sunlight reaches the surface of

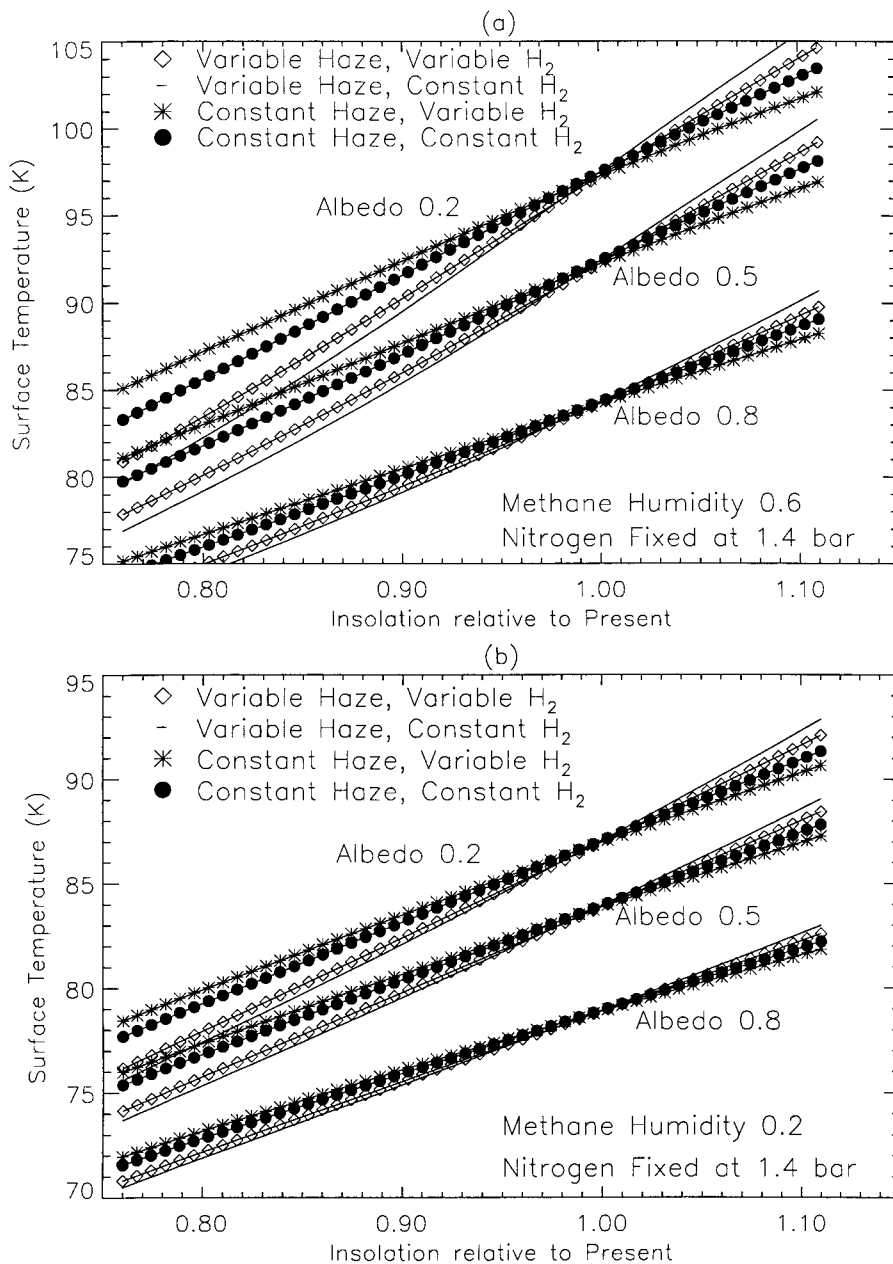


Fig. 3. Parametric sensitivity of surface temperature to solar evolution. (a) For methane humidities of 60%, (b) 20%. Hydrogen abundance and haze production are either held constant at present values described in the text, or scaled with time such that they are double their present values when the sun was 25% weaker in the past. It is seen that the enhanced greenhouse effect due to increased hydrogen abundance is insufficient to compensate for an enhanced antigreenhouse effect from the haze.

Titan that the surface temperature is not strongly sensitive to albedo. This range is also consistent with observational determinations of Titan's surface reflectivity. In the absence of haze (if the methane inventory were exhausted) the sensitivity to surface reflectivity is much higher (Lorenz et al., 1997b). Triton's albedo, by comparison, may be as high as 0.9 in places: we have studied albedos up to 0.8. Fig. 2 shows the dependence of surface temperature on surface albedo and methane humidity—for the observed methane abundance, our

semiempirical model indicates that values of surface albedo between 0.05 and 0.4 are appropriate to match the observed surface temperature, in agreement with the explicit numerical calculations in Lorenz et al. (1997b).

We have at all times assumed the surface has a thermal albedo of zero (and hence also an emissivity of 1). We used values of 0.8 to 2.0 bar for the nitrogen pressure: the radiative-convective model does not converge stably outside this range. In general,  $F_g$  has been kept

at zero in the present paper, although McKay et al. (1993, 1999) note that the atmosphere is very sensitive to geothermal heat flow—as may be seen from Eq. (4) above.

The solar flux has changed through time, due to the irreversible conversion of hydrogen to helium in its core. To describe the evolution of total solar luminosity, we use the formulation (Endal, 1980)  $S = S_0[1 + 0.4(1 - t/t_0)]^{-1}$  where  $S_0$  is the present solar constant and  $t_0$  is the age of the sun (4.6 Gyr). We do not concern ourselves with the first 1 Gyr of solar system history, when many other poorly-constrained factors would affect our model. First, the impactor flux on Titan would have been high and the satellite would still be shedding much of its heat of accretion (i.e. when the sun was not the only significant heat input to Titan's surface). Further, much of the  $N_2$  inventory may have been present as  $NH_3$ , the radiative effects of which we have not examined in our model (although see Kuramoto and Matsui, 1994, for a discussion.) Although the photochemical lifetime of ammonia is short, it might have been buffered by the initially-molten  $H_2O-NH_3$  surface and/or resupplied by ammonia-rich impactors.

The sun's spectrum has changed, as well as its total luminosity—some models indicate the sun has cooled and reddened as it has grown in size (and, indeed will continue to do so, becoming a red giant) Thus, the early sun, while faint, had a higher surface temperature and was therefore bluer. Zahnle and Walker (1982) note that at a solar age of 0.1 Gyr, the flux below about 200 nm was enhanced by 5–10 compared with present values, with EUV enhanced still more. In this paper, we assume that the flux, and therefore the haze production, vary as  $S^{-2}$ : hence 3.5 Gyr ago ( $S \sim 0.75$ ) the haze production rate was double. Gilliland (1989, Fig. 5) gives a similar relative value of 2.0 for the UV flux relative to current levels.

$P_H$  at present is 0.3–0.35. Values lower than 0.3 are incompatible with the observed geometric albedo of Titan (McKay et al., 1989). As haze production is photon-limited, we assume  $P_H$  is proportional to the UV flux, so  $P_H$  was higher in the past, enhancing the anti-greenhouse effect and reducing surface temperature further still.

$p_{H_2}$  is relatively small at present: taking Samuelson et al.'s (1997) estimate of a mixing ratio of 0.0011 gives a partial pressure of 0.0016. The hydrogen abundance is the result of the balance between photochemical production ( $\sim$ UV flux) and escape to space. To a first order, we assume then that the hydrogen mole fraction is proportional to the UV flux, and has the  $S$  dependence above: in the past, the UV flux and so the hydrogen abundance were higher, thereby increasing the hydrogen greenhouse effect and compensating in

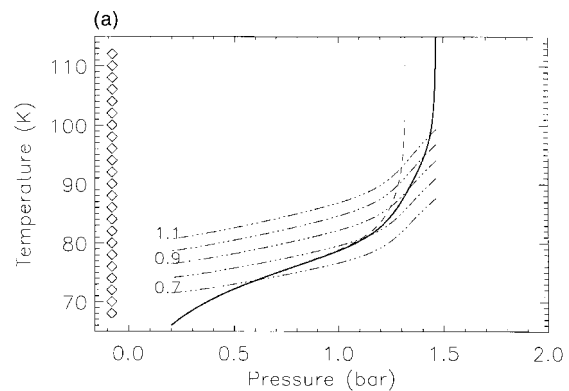


Fig. 4(a). Atmosphere–ocean equilibrium for the most volatile-poor Titan compatible with present-day observed atmosphere—0.1 bar ethane, 1.4 bar nitrogen and 0.2 bar methane. The solid line is the total pressure, and the dashed line the partial pressure of  $N_2$ , from the ocean thermodynamics. At any given temperature, then, the atmosphere has a fixed pressure and composition. That atmosphere produces a radiative equilibrium surface temperature shown by the dash-dot curves. The different curves correspond to different values of solar luminosity, e.g. the present day ( $S = 1.0$ ,  $P_H = 0.3$ ,  $p_{H_2} = 0.0016$  bar) curves for  $S = 0.7, 0.8$  and  $0.9$  and a future curve for  $S = 1.1$  are also shown. Where the dash-dot curves cross the thick solid line, the atmosphere–ocean system has an equilibrium (around 95 K and 1.4 bar for  $S = 1$ ) with the equilibrium moving smoothly to lower temperatures and pressures back in time as the sun grows fainter. This figure may be compared with Fig. 4 in McKay et al. (1993). The diamonds at the extreme left indicate that surface deposits are always liquid.

part for the enhanced antigreenhouse and lower solar constant.

Fig. 3 shows the variability of surface temperature as a function of these parameters. It can be seen that the variations in the haze antigreenhouse effect over time dominate the variations in the hydrogen greenhouse (as might be inferred from Figs. 2 and 3 of McKay et al., 1991). The fixed-humidity models shown in this figure, while illustrative of the various factors influencing surface temperature, are rather unphysical in terms of the equilibrium thermodynamics—they represent in effect a fixed  $N_2$  reservoir, all gaseous, and an infinite methane–ethane reservoir into which the  $N_2$  is not allowed to dissolve. This scenario was analyzed by McKay et al. (1993), who termed it ‘lakes’, in that it approximates Titan's present-day conditions if the hydrocarbon reservoir is modest (i.e. too small to dissolve much  $N_2$ , but enough to influence the  $CH_4$  humidity). A more realistic technique solves the equilibrium between a surface reservoir and the atmosphere for each species, using the algorithm outlined in an earlier section.

## 6. Self-consistent ocean-atmosphere equilibrium

We study the equilibrium of the ocean-atmosphere

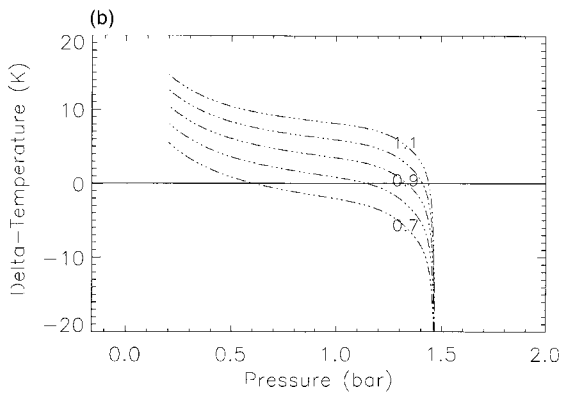


Fig. 4(b). The curves in (a) now shown with the thermodynamic equilibrium curve subtracted. All equilibria here are stable, since the radiative curves cross the zero line (the thermodynamic curve, thick line, in Fig. 4(a)) with a negative slope. As the sun evolves (moving from lower curves to upper) the crossing point moves smoothly to the right (higher pressure). If at any point the system is perturbed (e.g. by an impact boiling some ocean), the negative slope forces the system to return to the crossing point—a stable equilibrium.

system in the following manner. For a range of temperatures and a given volatile inventory, we compute the partial pressures of nitrogen and methane. The nitrogen partial pressure and the total pressure are plotted as dashed and solid lines, respectively, in Figs. 4(a) and 5(a). For each of these sets of partial pressures, we then use the radiative model to determine the surface temperature that would result from this atmosphere and various insolation values: these are plotted on the same figures as triple-dot-dashed curves. In general, these curves intersect the solid curve in one or more places.

As investigated by McKay et al. (1993), cases repre-

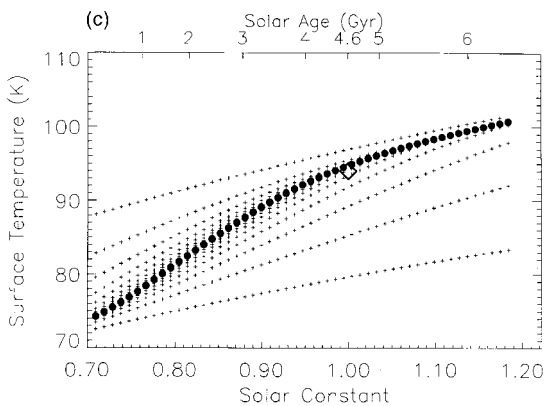


Fig. 4(c). Equilibrium surface temperature obtained by iterating the ocean and radiative models to determine the crossing points in (a) as a function of solar constant: small crosses are individual steps in the iterative process, and filled circles show the converged values. The temperature rise with increasing solar constant is smooth for this volatile-poor case. The thick diamond indicates present conditions. Upper scale shows solar age (present = 4.6 Gyr) assuming evolution model in the text.

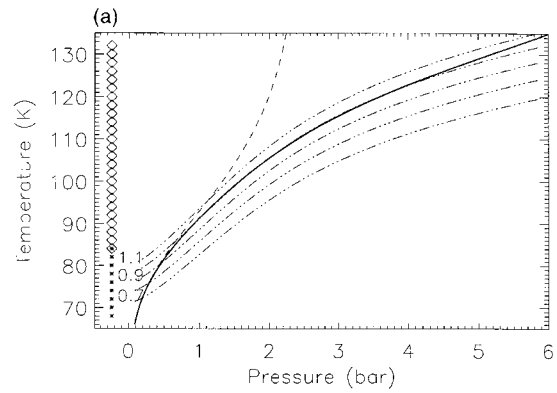


Fig. 5(a). (a) As in Fig. 4, but with a volatile-rich Titan (5.5 bar methane, 2.4 bar nitrogen and 6.5 bar ethane). This volatile inventory also produces an atmosphere at 94 K with roughly the pressure and composition of that observed today. The increased hydrocarbon abundance leads to partial freezing at rather higher-temperatures than for Fig. 4: totally-frozen surface deposits are indicated by the asterisks at left: diamonds indicate liquid surface reservoir, while both together indicate a partially frozen surface. Again, a stable equilibrium at present conditions is found, but note that the difference in slopes between the radiative and ocean equilibrium curves is small in (a) (indeed making the  $S = 1$  radiative curve difficult to discriminate from the thermodynamic curve shown by the thick line)—a small increase in insolation leads to a substantial increase in pressure: a runaway greenhouse is imminent.

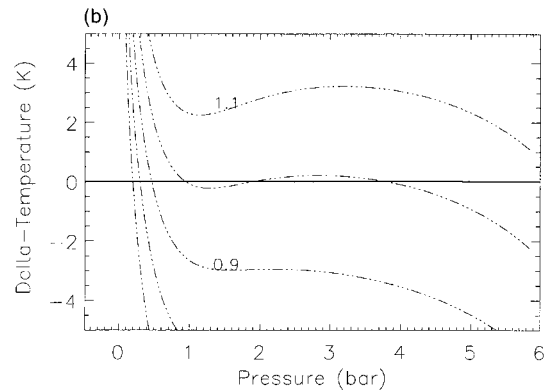


Fig. 5(b). The situation is made more clear in this figure, which magnifies the difference between the curves in (a) by subtracting the thermodynamic equilibrium curve (as in 4(b)). Three equilibria are found, with pressures of 1.0, 1.9 and 3.8 bar: a very small change in the parameters would yield a pressure of 1.4 bar exactly, although here the parameters are tuned slightly to show more clearly the triple equilibrium. As the sun evolves, moving from the lower curves to the upper, two more equilibria appear: the leftmost is stable and is equivalent to the original single low pressure equilibrium. The center crossing has a positive slope and is therefore unstable. If the system is perturbed (e.g. a temporary pressure increase) by a small amount, it will return to the original, leftmost, equilibrium. If the system is perturbed significantly, beyond the center crossing, it will instead converge on the rightmost (high pressure) equilibrium—a runaway greenhouse. As the sun evolves and the curve move upwards, the stability margin decreases and the perturbation required to ‘flip’ the system becomes smaller. Ultimately the two leftmost crossings vanish and the system, having nowhere else to go, jumps to the high pressure equilibrium.

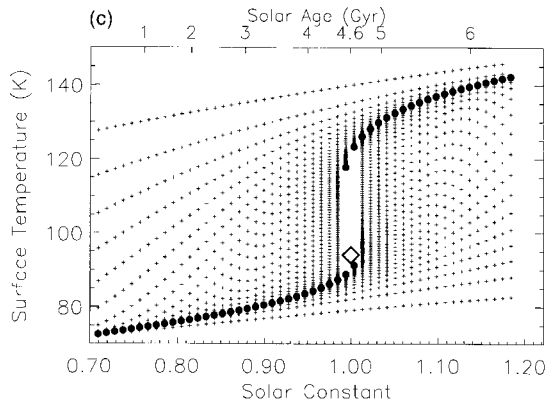


Fig. 5(c). The runaway greenhouse is apparent in this volatile-rich case. Note also the large number of iterations required to converge, and the near convergence at  $S = 1.01$  before the system runs away to a higher-temperature equilibrium. Some hysteresis is evident—turning the sun back down in intensity does not collapse the system back to the low-temperature state until  $S < 0.98$ .

sentative of Titan's present atmosphere (with about 60% methane relative humidity) have a stable equilibrium. [This is not a surprise; if the equilibrium were unstable, we are unlikely to observe that state in nature.] In these cases the radiative (triple-dot-dash curve) has a more negative slope than the ocean equilibrium curve where they cross (the radiative curve crosses in a left-right downgoing sense: for a given temperature the ocean produces a gas mixture whose radiative equilibrium temperature is somewhat higher, so the ocean warms up (moving up the curve, to the right). This in turn produces a gas mixture with a higher equilibrium temperature, but the temperature increment corresponding to this pressure increase is less than that required to produce it. So eventually the curves march upward until they meet.

The relative slopes are more evident in Figs. 4(b) and 5(b)—negative slopes imply a stable equilibrium. It can be seen in Fig. 5(b) that a volatile-rich case acquires an additional stable state as the sun evolves (a third equilibrium appears between them, but is not stable). Environmental perturbations (e.g. geothermal heating, or impact boiling of part of the reservoir), if sufficient to push the system beyond this unstable equilibrium, could flip the system between the two stable equilibria. Depending on the original state, the 'flip' can be regarded as an atmosphere 'collapse' or a runaway greenhouse. Ultimately, as the sun increases in luminosity, the low-temperature/low pressure equilibrium disappears.

The equilibrium temperatures where the radiative and ocean curves converge are shown as a function of solar constant for various volatile inventories in Figs. 4(c) and 5(c): an initial temperature of 70 or 150 K is set, and the atmosphere computed. This atmosphere is then passed through the radiative model, to compute a

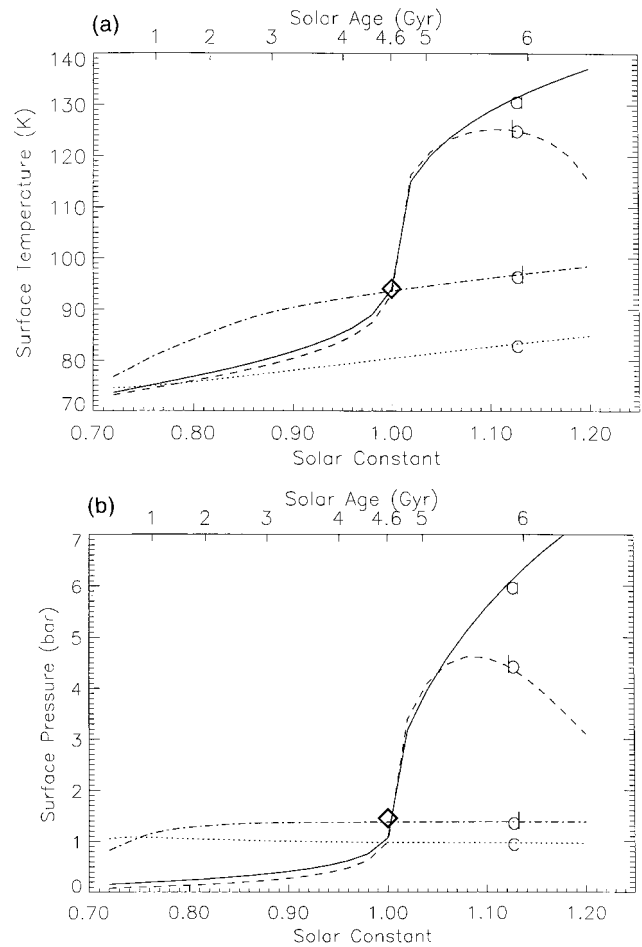


Fig. 6. Coupled evolution calculations. The top panel shows surface temperature and the bottom shows surface pressure. The diamond indicates present conditions. The cases (a)–(d) are described in the text: volatile-rich cases (a) and (b) show the potential for dramatic warming in the near future—a runaway greenhouse—while the volatile-poor cases (c) and (d) show a more gradual warming as solar luminosity increases. Case (c) is incompatible with present conditions.

new temperature, and the process repeated until the temperature converges to within 0.01 K. The individual iterations are shown as crosses, and the converged values by filled circles. It is found that for volatile-rich cases, there is hysteresis in the climate system, and two equilibrium temperatures for a given solar constant exist, depending on whether a low- or high-temperature state is used as the starting point. This is essentially the same effect as has been noted for the runaway greenhouse on Earth (Nakajima et al., 1992).

Note that the present model does not address the 'hard' collapse of the atmosphere to 100 mbar and below (Lorenz et al., 1997b) when atmospheric methane is exhausted—this in part because our opacity formulation breaks down for very low methane abundances, and in part because the present study considers surface temperatures only, and does not take into

account possible cooling higher in the atmosphere leading to nitrogen rainout. If the methane were ever depleted completely, such a collapse in temperature and pressure could occur, and the stability of the climate of the now pure nitrogen atmosphere could be considered in an analogous way to that above.

## 7. Coupled evolution calculations

We now apply the iterative coupled surface-atmosphere models to examine the effects of combining the evolution of the volatile inventory (photolysis and/or delivery of methane) with solar evolution (increasing solar constant, and falling UV flux).

Note that as many as 200 iterations are required at each timestep (i.e. solar constant value) to converge to within 0.01 K of a self-consistent surface-atmosphere equilibrium: without using the analytic formulation to approximate the results of the numerical radiative transfer code, these calculations would take prohibitively long.

The results are summarized in Fig. 6 and discussed below.

1. Case (a): This case has an initial (3 bar) nitrogen inventory, and 10.8 bar of CH<sub>4</sub>. Over the 4 Gyr to the present, 6 bar of ethane accumulates; the methane inventory is held constant—it is assumed to be replenished as fast as it is destroyed. This case has a cold, low-pressure early history, as the large methane reservoir dissolves most of the atmospheric nitrogen. Around the present epoch, a runaway greenhouse occurs and most of the liquid reservoir evaporates.
2. Case (b): This case is essentially the canonical Titan ocean explored by Lunine et al. (1983), Dubouloz et al. (1989), etc. An initial inventory of 25 bar of methane is slowly converted into ethane, at the same rate as above. No replenishment occurs. Thus, since methane was slightly more abundant early in the history, the early temperatures and pressures are slightly lower—the larger ocean can dissolve more of the 3 bar of nitrogen from the atmosphere. Again, at the present epoch, runaway occurs, but the atmosphere deflates in the future when the methane is exhausted by photolysis.
3. Case (c): This is a volatile-poor version of case (a): the minimum inventory of methane and nitrogen (0.1 and 1.4 bar) compatible with the present day are held constant, i.e. methane is resupplied as fast as it is destroyed. Again 6 bar of ethane accumulates by the time the solar constant reaches 1.0 at the present: this is enough to dissolve out most of the methane, so temperatures stay low. This model

is not compatible with the observed temperature and pressure on Titan.

4. Case (d): This is case (c), with the exception that no ethane accumulates (in geological terms, one may imagine that it is, for example, subducted and removed from the surface-atmosphere equilibrium). Because there is only 1.5 bar of volatiles, these reside throughout time mostly in the gas phase, producing the Titan atmosphere we observe today and a pressure only slightly smaller in the past. Since most of the volatiles are already in the gas phase, there is no strong positive feedback on warming, so the future evolution is very small.

## 8. Conclusions

We have studied self-consistent surface-atmosphere climate equilibrium on Titan using a new semiempirical grey radiative model. This model may be applied to other bodies with thick absorbing atmospheres.

We have found that the climate has hysteresis for large volatile inventories with respect to insolation (and, by implication, geothermal heating—see McKay et al. (1999)): two stable equilibria are found for single values of these parameters, depending on the initial conditions. A volatile-rich scenario of Titan may have entailed a collapse from an initial methane-rich atmosphere warmed by enhanced geothermal heating (heat of accretion) to a low pressure, low temperature state that only recently warmed by an accelerating greenhouse effect. Future evolution of surface temperatures depends on the present-day volatile inventory: a volatile-poor scenario will warm only gradually, while a volatile-rich one may rise rapidly in temperature and pressure.

If Titan does have a large endowment of volatiles, then calculations of Titan's climate in the far future that ignore positive greenhouse feedback (Lorenz et al., 1997b) may be pessimistic—Titan may warm up to the point where ammonia-doped surface ices may melt rather sooner than those models predict.

Titan's climate in the past and future may be inferred Cassini observations: geomorphologies associated with widespread surface liquids may be evident, and the effect of a thinner past atmosphere may be apparent from crater size-distribution considerations (Engel et al., 1995; Ivanov et al., 1997). While observations coupled with our models could be used to deduce the existence of a large volatile inventory, much of that inventory may not be directly observable, but be in a subsurface reservoir.

In general, as noted by McKay et al. (1993), Titan's atmosphere would have had a lower pressure in the past, even if the volatile inventory were constant.

However, if the nitrogen inventory has stayed constant, and methane resupply did not keep pace with photolysis, there have been methane-poor periods, when more nitrogen would be forced out of the ocean and the pressure and temperature could have been higher—again this may be apparent in the crater-size distribution. On the other hand, if methane were at times exhausted completely as discussed in Lorenz et al. (1997), a low-pressure, low-temperature state may have prevailed for much of Titan's history.

One intriguing scenario is that no evidence for a large volatile reservoir is found. This would imply either of two possibilities: either methane is a recent introduction to the surface-atmosphere system, suggesting that a search for volcanic features may prove fruitful, or somehow ethane is removed from the equilibrium, in which case trenches or subduction zones may be a feature of Titan's crust.

Global mapping observations by Cassini, by radar and by viewing through atmospheric windows in the near-infrared using the ISS (Imaging Science Subsystem) and VIMS (Visual and Infrared Mapping Spectrometer) instruments should indicate the global distribution of liquid (or at least organic) deposits on Titan at modest resolution, giving at least a crude measure of the volatile inventory. These instruments will also search for geomorphological features connecting the atmosphere with the interior such as the volcanic features and subduction zones mentioned above. Energetic particle flux measurements, and direct sampling of the upper atmosphere with the Ion and Neutral Mass Spectrometer (INMS) will constrain present-day atmospheric escape processes.

Measurements from remote sensing instruments, but in particular from the Gas Chromatograph-Mass Spectrometer on the Huygens probe, will improve the constraints on isotopic ratios, and introduce new quantities (unmeasurable from Earth) such as the noble gas abundances and isotope ratios. Isotope ratios of krypton and xenon are directly diagnostic of the amount of atmospheric escape, while argon isotope ratios should constrain the amount of outgassing from the interior.

All these measurements, taken together, will give us a clearer picture of Titan's atmospheric history, and, perhaps, its potentially volatile climatic future.

### Acknowledgements

R.D.L. acknowledges the support of the Cassini Project. JIL and CPM acknowledge the support of the NASA Planetary Geology and Atmospheres programs. JIL is grateful to Angioletta Coradini for hosting his stay at CNR-IAS during the preparation of the paper. We thank Bob Samuelson for an encouraging and con-

structive review of an earlier version of this paper. Referees Jim Kasting and Emmanuel Lellouch are thanked for their useful comments.

### References

- Courtin, R., Gautier, D., McKay, C.P., 1995. Titan's thermal emission spectrum: re-analysis of the voyager infrared measurements. *Icarus* 114, 144–162.
- Dubouloz, N., Raulin, F., Lellouch, E., Gautier, D., 1989. Titan's hypothesized ocean properties: the influence of surface temperature and atmospheric composition uncertainties. *Icarus* 82, 81–96.
- Eluskiewicz, J., Stevenson, D.J., 1990. Physico-chemical state of Titan's subsurface layers. *Lunar and Planetary Science Conference XXI*, 323–324 (abstracts).
- Endal, A.S., 1980. Evolutionary variations of solar luminosity. In: *Variations of the Solar Constant*, NASA Conference Publication CP-2191, Goddard Space Flight Center, Maryland, November 5–7, pp. 175–181.
- Engel, S., Lunine, J.I., Hartmann, W.K., 1995. Cratering on Titan and implications for Titan's atmospheric history. *Planetary and Space Science* 43, 1059–1066.
- Flasar, F.M., 1983. Oceans on Titan? . *Science* 221, 55–58.
- Gibbard, S.G., Macintosh, B., Gavel, D., Max, C.E., De pater, I., Ghez, A.M., Young, E.F., McKay, C.P. 1999 Titan: high resolution speckle images from the Keck telescope. *Icarus*, in press.
- Gilliland, R.L., 1989. Solar evolution. *Palaeogeography, Palaeoclimatology, Palaeoecology* 75, 35–55.
- Ingersoll, A., 1969. The runaway greenhouse: a history of water on Venus. *J. Atmospheric Sciences* 26, 1191–1198.
- Ivanov, B.A., Basilevsky, A.T., Neukum, G., 1997. Atmospheric entry of large meteoroids: implication to Titan. *Planetary and Space Science* 45, 993–1007.
- Kasting, J.F., Pollack, J.B., Ackerman, T.P., 1988. Response of earth's atmosphere to increases in solar flux and implications for loss of water from Venus. *Icarus* 57, 335–355.
- Kossacki, K.J., Lorenz, R.D., 1996. Hiding Titan's ocean: densification and hydrocarbon transport in an icy regolith. *Planetary and Space Science* 44, 1029–1037.
- Kouvaris, L.C., Flasar, F.M., 1991. Phase equilibrium of methane and nitrogen at low temperatures: application to Titan. *Icarus* 91, 112–124.
- Kuramoto, K., Matsui, T., 1994. Formation of a hot proto-atmosphere on the accreting giant icy satellite: implications for the origin and evolution of Titan, Ganymede and Callisto. *J. Geophys. Res.* 99, 21,183–21,200.
- Lara, L.M., Lellouch, E., Lopez-Moreno, J.J., Rodrigo, R., 1996. Vertical distribution of Titan's atmospheric neutral constituents. *J. Geophys. Res.* 101, 23,261–23,283.
- Lara, L.M., Lorenz, R.D., Rodrigo, R., 1994. Liquids and solids on the surface of Titan: results of a new photochemical model. *Planetary and Space Science* 42, 5–14.
- Lellouch, E., Coustenis, A., Raulin, F., Dubouloz, N., Frere, C., 1989. Titan's atmosphere and hypothesized ocean: a reanalysis of Voyager 1 radio-occultation and IRIS 7.7  $\mu\text{m}$  data. *Icarus* 79, 328–349.
- Lindal, G.F., Wood, G.E., Hotz, H.B., Sweetnam, D.N., Eshleman, V.R., Tyler, G.L., 1983. The atmosphere of Titan: an analysis of the Voyager 1 radio occultation measurements. *Icarus* 53, 348–363.
- Lorenz, R.D., 1998. Many lakes make an ocean: constraining Titan's volatile inventory. In: *Lunar and Planetary Science Conference (abstracts on CD-ROM)*, XXIX, Houston, March.
- Lorenz, R.D., Lunine, J.I., 1997. Titan's surface reviewed: the nature

- of bright and dark terrain. *Planetary and Space Science* 45, 981–992.
- Lorenz, R.D., Lunine, J.I., McKay, C.P., 1997a. Titan under a red giant sun: a new kind of ‘habitable’ moon. *Geophysics Research Letters* 24, 2905–2908.
- Lorenz, R.D., McKay, C.P., Lunine, J.I., 1997b. Photochemically-driven collapse of Titan’s atmosphere. *Science* 275, 642–644.
- Lunine, J.I., Rizk, B., 1989. Thermal evolution of Titan’s atmosphere. *Icarus* 80, 370–389.
- Lunine, J.I., Stevenson, D.J., 1985. Evolution of Titan’s coupled ocean-atmosphere system and interaction of ocean with bedrock. In: Klinger, J., Benest, D., Dollfus, A., Smoluchowski, R. (Eds.), *Ices in the Solar System*. Reidel, Dordrecht, The Netherlands, pp. 741–757.
- Lunine, J.I., Yung, Y.L., Lorenz, R.D. 1999 On the volatile inventory of Titan from isotopic abundances in nitrogen and methane. *Planetary and Space Science*, in press.
- Lunine, J.I., Stevenson, D.J., Yung, Y.L., 1983. Ethane ocean on Titan. *Science* 222, 1229–1230.
- McKay, C.P., Lorenz, R.D., Lunine, J.I., 1999. Analytic solutions for the antigreenhouse effect: Titan and the early earth. *Icarus* 137, 56–61.
- McKay, C.P., Martin, S.C., Griffith, C.A., Keller, R.M., 1997. Temperature lapse rate and methane in Titan’s atmosphere. *Icarus* 129, 498–506.
- McKay, C.P., Pollack, J.B., Lunine, J.I., Courtin, R., 1993. Coupled atmosphere-ocean models of Titan’s past. *Icarus* 102, 88–98.
- McKay, C.P., Pollack, J.B., Courtin, R., 1991. The greenhouse and anti-greenhouse effect on Titan. *Science* 253, 1118–1121.
- McKay, C.P., Pollack, J.B., Courtin, R., 1989. The thermal structure of Titan’s atmosphere. *Icarus* 80, 23–53.
- Muhlemann, D.O., Grossman, A.W., Butler, B.J., 1995. Radar investigations of Mars, Mercury and Titan. *Annual Review of Earth and Planetary Sciences* 23, 337–374.
- Nakajima, S., Hayashi, Y.-Y., Abe, Y., 1992. A study on the ‘Runaway Greenhouse Effect’ with a one-dimensional radiative-convective model. *J. Atmos. Sciences* 49, 2256–2262.
- Samuelson, R.E., 1983. Radiative equilibrium model of Titan’s atmosphere. *Icarus* 53, 364–387.
- Samuelson, R.E., Rath, N.R., Borysow, A., 1997. Gaseous abundances and methane supersaturation in Titan’s troposphere. *Planetary and Space Science* 45, 959–980.
- Smith, P.H., Lemmon, M.T., Lorenz, R.D., Caldwell, J.J., Allison, M.D., Sromovsky, L.A., 1996. Titan’s surface, revealed by HST imaging. *Icarus* 119, 336–349.
- Strobel, D.F., Hall, D.T., Zhu, X., Summers, M.E., 1993. Upper limit on Titan’s atmospheric argon abundance. *Icarus* 103, 333–336.
- Thompson, W.R., 1985. Phase equilibria in N<sub>2</sub>-hydrocarbon systems: applications to Titan. In: *The Atmospheres of Saturn and Titan. Proceedings of the International Workshop, Alpbach, Austria, September*, pp. 109–119 ESA SP-241.
- Thompson, W.R., Zollweg, J.A., Gabis, D.H., 1992. Vapor-liquid equilibrium thermodynamics of N<sub>2</sub> + CH<sub>4</sub>: model and Titan applications. *Icarus* 97, 187–199.
- Toublanc, D., Parisot, J.P., Brillet, J., Gautier, D., Raulin, F., McKay, C.P., 1995. Photochemical modelling of Titan’s atmosphere. *Icarus* 113, 2–26 (see also erratum 117, 218).
- Yelle, R.V., Strobel, D.F., Lellouch, E., Gautier, D., 1997. Engineering models for Titan’s atmosphere. In: *Huygens Science, Payload and Mission. European Space Agency SP-1177*, Noordwijk, The Netherlands, August.
- Yung, Y.L., Allen, M., Pinto, J.P., 1984. Photochemistry of the atmosphere of Titan: comparison between model and observations. *Astrophys. J. Suppl.* 55, 465–506.
- Zahnle, K., Walker, J.C.G., 1982. Evolution of solar ultraviolet luminosity. *Rev. Geophysics* 20, 280–292.